IAEA
International Atomic Energy Agency

INDC(ITY)-0018
Distr. G

INDC International Nuclear Data Committee

Activity Report of the ENEA Nuclear Data Project in 2010

Prepared by

Alberto Ventura

Centro di Ricerche Ezio Clementel
Via Martiri di Monte Sole 4
40129 Bologna, ITALY

September 2011

IAEA Nuclear Data Section, Vienna International Centre, A-1400 Vienna, Austria

Selected INDC documents may be downloaded in electronic form from
http://www-nds.iaea.org/reports-new/indc-reports/
or sent as an e-mail attachment.
Requests for hardcopy or e-mail transmittal should be directed to
services@iaeand.iaea.org
or to:

Nuclear Data Section
International Atomic Energy Agency
Vienna International Centre
PO Box 100
A-1400 Vienna
Austria

Printed by the IAEA in Austria

September 2011

INDC(ITY)- 0018
Distr. G

Activity Report of the ENEA Nuclear Data Project in 2010

Prepared by
Alberto Ventura
Centro di Ricerche Ezio Clementel
Via Martiri di Monte Sole 4
40129 Bologna, ITALY

Abstract

Descriptions are given of the nuclear data activities undertaken during 2010 at the Bologna Research Centre of the Italian National Agency for New Technologies, Energy and Sustainable Economic Development (ENEA).

September 2011

TABLE OF CONTENTS

General Quantum Mechanics

Group-theoretical treatment of the quantum Coulomb-Rosochatius system

The Schrödinger equation for a non-relativistic spinless particle of mass *m* moving under the effect of a three-dimensional Coulomb-Rosochatius potential

$$V(x,y,z) = -\frac{\gamma}{r} + \frac{\beta_x}{2x^2} + \frac{\beta_y}{2y^2} + \frac{\beta_z}{2z^2}$$

where $r = \sqrt{x^2 + y^2 + z^2}$ and γ , β_x , β_y and β_z are real constants, lends itself to a group-theoretical derivation of bound and scattering states within the framework of the potential group approach.

In analogy with the three-dimensional Coulomb potential, which admits *SO(4)* and *SO(3,1)* as symmetry groups for bound states and scattering states, respectively, the non-central Coulomb-Rosochatius potential admits *SO(7)* and *SO(6,1)* as potential groups for bound and scattering states, respectively, if $\beta_i = s_i^2 - \frac{1}{4}, (i = x, y, z)$, with s_i integer numbers, as shown in Ref. [A.1], where, in addition, the *S*-matrix elements for elastic scattering are computed by the method of intertwining operators.

The approach lends itself to a generalization to *n* dimensions, where the potential groups are conveniently chosen as *SO(3n+1)* and *SO(3n,1)* for bound states and scattering states, respectively [C.1].

Reflectionless PT-symmetric potentials in the one-dimensional Dirac equation

In the family of PT-symmetric potentials, *i.e.* complex potentials that are invariant under the product, PT, of parity P and time reversal T, but not under P and T separately, reflectionless potentials play a peculiar role, because they do not break unitarity and their asymptotic scattering wave functions, as well as their bound-state wave functions, are eigenstates of PT.

Ref. [A.2] studies bound states and scattering states of solvable reflectionless potentials in the Dirac equation in one spatial dimension with different covariance properties: scalar-plus-vector, pure scalar and pseudoscalar. The two last cases are of particular interest, because it is possible to define a P-pseudo-supersymmetry where either the scalar potential plus the particle mass, or the pseudoscalar potential play the role of superpotential: examples are given where the pseudo-supersymmetry is either exact or spontaneously broken. In the former case the discrete spectra of the two supersymmetry partners differ by one state, in the latter they coincide.

Nuclear Reaction Theory and Experiments

Measurements of neutron cross sections at the n_TOF facility, CERN

The second experimental campaign, started in 2008, continued in 2010, with measurements of neutron radiative capture and neutron-induced fission.

Capture measurements were focused on *Fe* and *Ni* isotopes, with particular reference to $^{56,56}Fe$ and ^{62}Ni, and on ^{241}Am, using both $C_6 D_6$ detectors and total absorption calorimeter. As for fission, angular distributions of fission fragments of ^{232}Th, $^{235,238}U$ and ^{237}Np were measured by means of parallel-plate avalanche counters.

Several analyses of radiative capture cross sections measured during the first experimental campaign (2002-2004) were published in 2010: they include:

1) $^{92}Zr(n,\gamma)$ in the resolved resonance region (E_n < 40 keV) [A.3] : this cross section is important both to the *s*-process in stellar nucleosynthesis and to nuclear technology applications : an accurate determination of this cross section is relevant also to the study of transmutation of the long-lived fission product ^{93}Zr by neutron capture. The measurement, performed with two C_6D_6 detectors, provided a set of improved parameters for 44 resonances in the quoted energy range. With this information the cross section uncertainties in the keV region were reduced to 5%, as required in astrophysical and technological applications.
2) $^{197}Au(n,\gamma)$ in the resolved resonance region (E_n < 5 keV) [A.4]: as is known, the $^{197}Au(n,\gamma)$ reaction at thermal energy and in the interval from 0.2 to 2.5 MeV is a capture standard and most neutron-capture cross-section measurements refer to one or to both energy regions. The aim of the n_TOF measurement is to improve the accuracy in an energy region where it is not yet considered standard, with particular reference to the resolved energy region, where relatively few measurements exist. Use was made of two different experimental setup and detection techniques, the total energy method based on C_6D_6 detectors, and the total absorption calorimetry based on a 4π BaF_2 array. 273 resonances were observed between 4.9 eV and 5 keV, some of them for the first time.
3) $^{186,187,188}Os(n,\gamma)$ from 1 eV to 1 MeV: the precise measurement of the neutron capture cross sections of ^{186}Os and ^{187}Os is relevant to the definition of the *s*-process abundance of ^{187}Os at the formation of the solar system. This quantity can be used to evaluate the radiogenic component of the abundance of ^{187}Os due to the decay of ^{187}Re ($t_{1/2}$ = 41.2 Gyr) and to infer from this the duration of the nucleosynthesis in our galaxy (*Re/Os* cosmochronometer). The measurements were performed at the n_TOF facility with the total energy method based on two $C_6 D_6$ detectors. The capture cross sections in the unresolved resonance region up to 1 MeV are described in Ref. [A.5] and presented in Fig. 1a-c. The resolved region is described in Ref. [A.6]: in total, 186, 480 and 199 resonances were identified up to 5, 3 and 8 keV for ^{186}Os, ^{187}Os and ^{188}Os, respectively. On the basis of statistical model calculations, stellar enhancement factors were obtained to correct the Maxwellian averaged cross sections determined from experimental capture data for the effect of thermally excited states in the hot photon bath at the *s*-process site. The corresponding stellar *(n,γ)* cross sections were used to separate the radiogenic part of the ^{187}Os abundance from its *s*-process component and to define the mother/daughter ratio $^{187}Re/^{187}Os$.

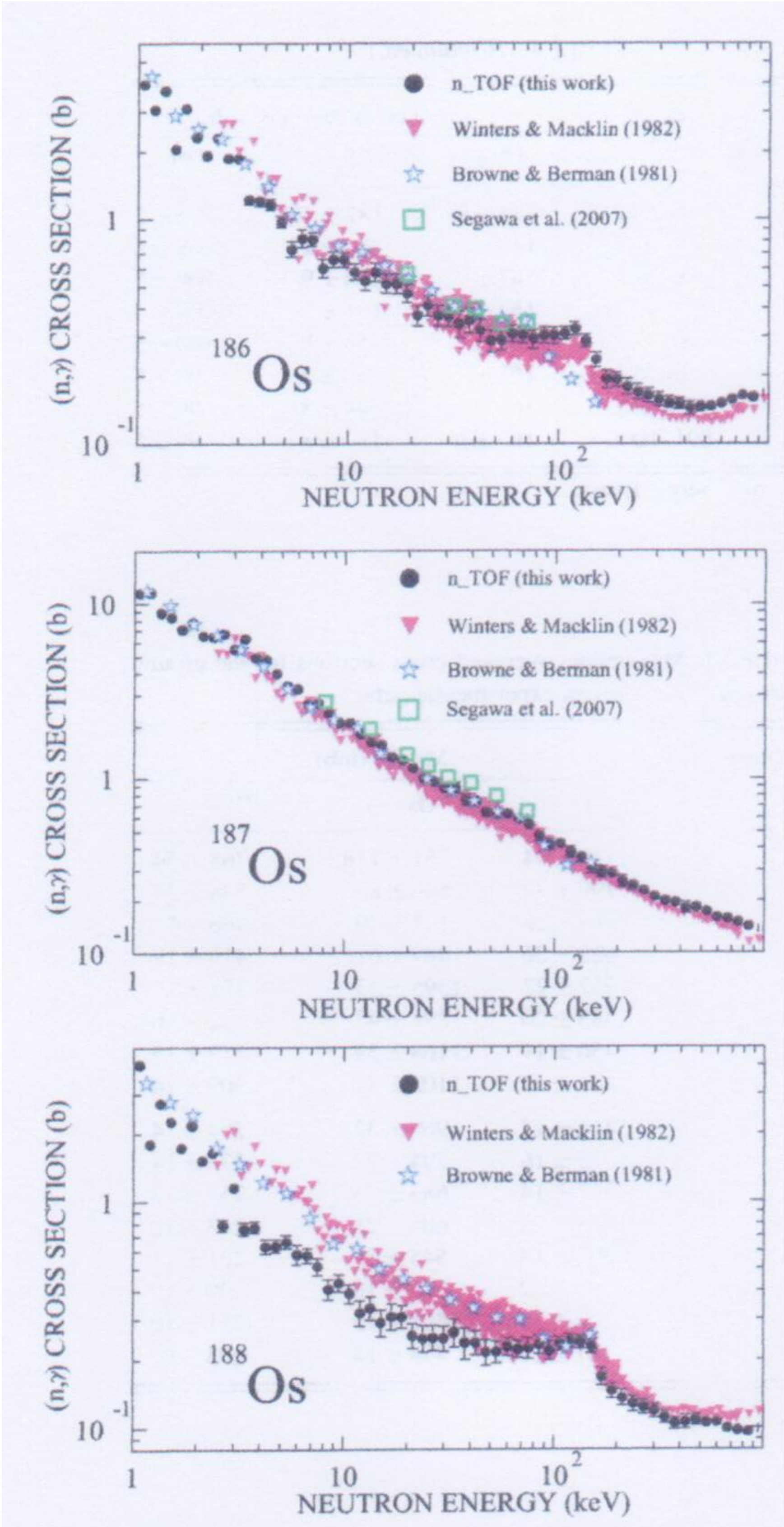

Fig. 1. Radiative capture cross sections of $^{186,187,188}Os$ in the unresolved resonance region.

The fission measurements published in 2010 [A.7] are the cross sections of ^{234}U and ^{237}Np [C.2] in a broad energy range, from ~ 1 eV to ~ 1 GeV. These isotopes were chosen because ^{234}U plays an important role in the *U/Th* fuel cycle, while ^{237}Np is one of the more abundant isotopes in the spent fuel from current reactors.

The measurements, relative to the fission cross section of ^{235}U in the same energy range, were performed with a reaction chamber based on parallel-plate avalanche counters. The data obtained for ^{234}U are in overall good agreement with previous measurements and evaluations in the continuum, as shown in Fig. 2. Differences exist in the resolved resonance region, where there is a lack of recent experimental data.

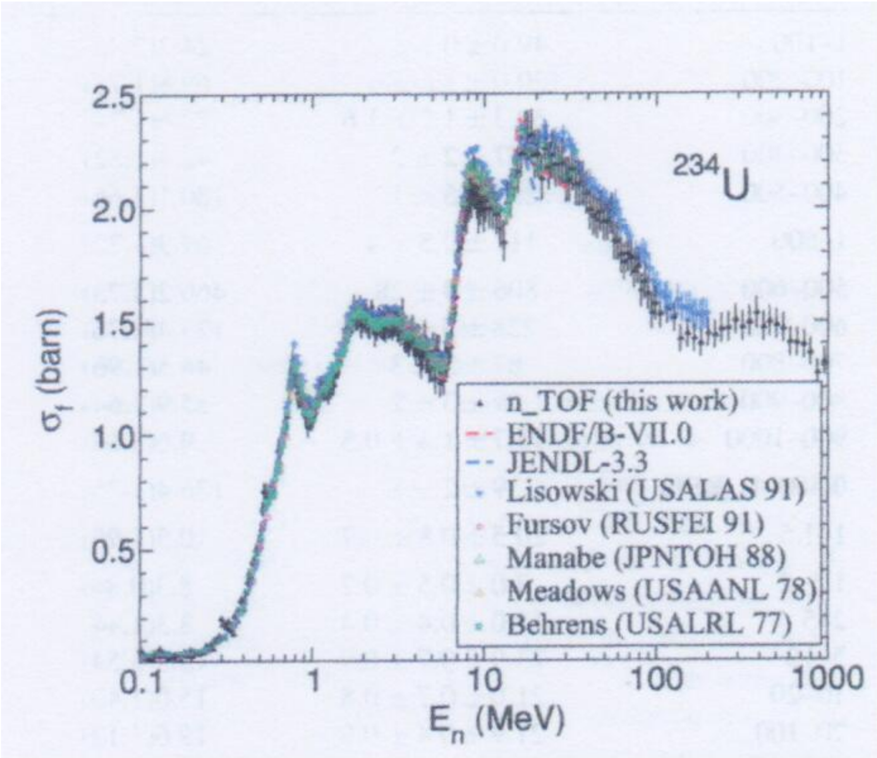

Fig. 2. Neutron-induced fission cross section of ^{234}U from threshold up to 1 GeV.

On the other hand, the n_TOF data of ^{237}Np exhibit significant discrepancies with recent evaluations, although the cross-section shape is quite similar: in particular, the data are systematically higher than ENDF/B-VII.0 by ~3% below and 6% above 1 MeV. Even larger differences of 8% are found above 6 MeV with respect to JENDL-3.3, significantly beyond the 3%-4% systematic uncertainty of the n_TOF data. The agreement is better in the resolved resonance region. A comparison of data and evaluations from threshold up to 1 GeV is shown in Fig. 3.

Simulations of an integral experiment performed to verify the measured fission cross section indicate that the effective multiplication coefficient that was measured is well reproduced if the n_TOF data are used instead of ENDF/B-VII.0.

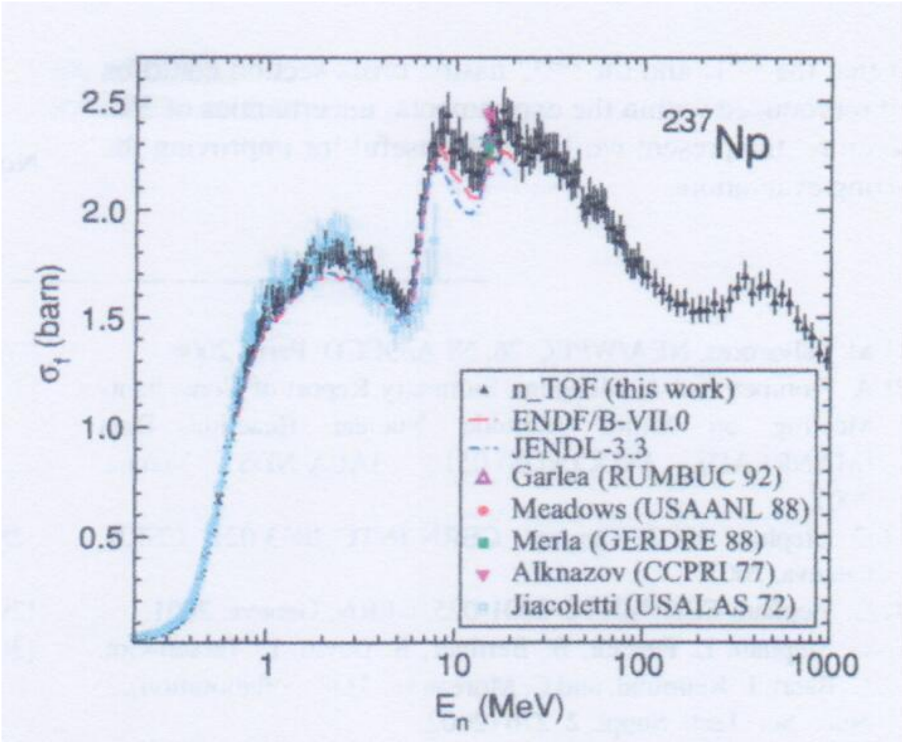

Fig. 3. Neutron-induced fission cross section of ^{237}Np from threshold up to 1 GeV.

Descriptions of the present status of the n_TOF facility [C.3] and of the new neutron beam [C.4] were presented at the international conference on Nuclear Data for Science and Technology, held at the Jeju Island, Korea, from 26 to 30 April 2010. Preliminary results of other capture [C.5],[C.6],[C.7] and fission [C.8],[C.9] measurements were presented at the same conference; among the latter, Fig. 4 from Ref. [C.8] shows the data obtained for ^{243}Am, which disprove the results of a recent experiment and agree with previous measurements and evaluations.

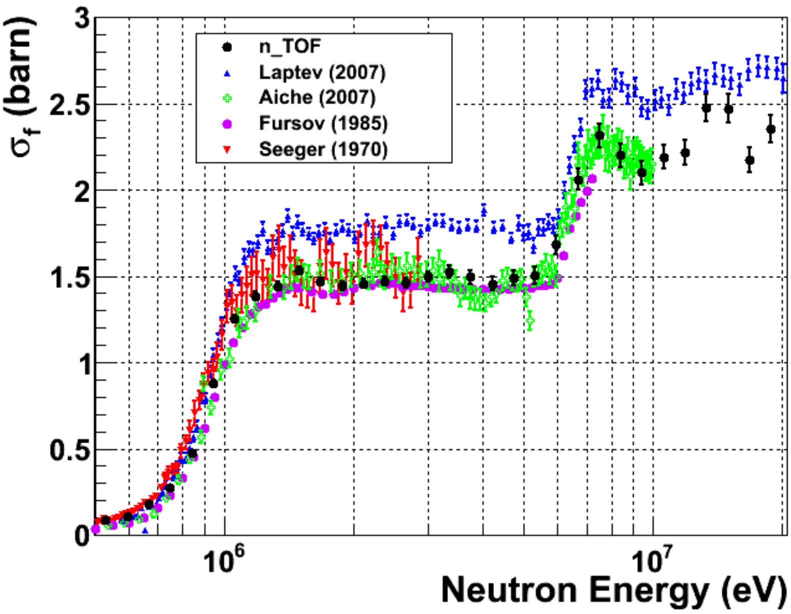

Fig. 4. Neutron-induced fission cross section of ^{243}Am.

Finally, the relevance of n_TOF data to the design of innovative reactors is discussed in Ref. [A.8].

Nuclear Data Processing and Validation

Proper reporting of the nuclear data processing and validation activities performed in 2009 was started. In addition data validation activities, dedicated to the ENEA-Bologna BUGJEFF311.BOLIB broad-group (47 neutron groups + 20 photon groups) coupled neutron and photon working cross section library in FIDO-ANISN format, were performed. The BUGJEFF311.BOLIB library, obtained through problem-dependent cross section collapsing of the ENEA-Bologna VITJEFF311.BOLIB fine-group (199 neutron groups + 42 photon groups) coupled neutron and photon cross section library for fission applications (based on the JEFF-3.1.1 evaluated data library), is specifically dedicated to LWR shielding and pressure vessel dosimetry applications. The cross section collapsing mentioned was performed with the updated and corrected ENEA-Bologna 2007 Revision of the ORNL SCAMPI nuclear data processing system. It is worth stressing, on the other hand, that the ENEA-Bologna BUGJEFF311.BOLIB library and the ENEA-Bologna 2007 Revision of the ORNL SCAMPI nuclear data processing system are now in regular free distribution at the OECD-NEA Data Bank.

The BUGJEFF311.BOLIB library was tested in particular on the PCA-Replica 12/13 (Winfrith, UK) and VENUS-3 (Mol, Belgium) engineering neutron shielding benchmark experiments, included in the international SINBAD database of reactor shielding experiments. These integral benchmark experiments were specifically conceived to check the nuclear data and the transport codes used in LWR radiation shielding and radiation damage analyses. Three-dimensional fixed source transport calculations were performed with the three-dimensional TORT-3.2 discrete ordinates (S_N) code for both the cited benchmark experiments.

The calculated results obtained with BUGJEFF311.BOLIB for the PCA-Replica 12/13 and VENUS-3 benchmark experiments were compared not only with the corresponding experimental values but also with similar ENEA-Bologna results obtained, with the same calculation methodology, through the well known ORNL BUGLE-96 similar library, based on ENDF/B-VI.3 nuclear data.

The PCA-Replica neutron shielding benchmark experiment is a water/iron benchmark experiment including PWR thermal shield and pressure vessel simulators. The source of neutrons is a thin fission plate (whose dimensions are 63.5 cm × 40.2 cm × 0.6 cm) of highly enriched uranium (93.0 w% in U-235), irradiated by the NESTOR low-power experimental reactor through a graphite thermal column (total thickness 43.91 cm). Beyond the fission plate, the PCA-Replica shielding array (12/13 experimental configuration with two water gaps of about 12 cm and 13 cm) was arranged in a large parallelepiped steel tank (square section; side 180.0 cm) filled with water. After a first water gap (12.1 cm), there was the stainless steel thermal shield simulator (5.9 cm), the second water gap (12.7 cm), the mild steel pressure vessel simulator (thickness T = 22.5 cm) and a wide box made of a thin layer of aluminium simulating the air cavity between the pressure vessel and the biological shield in a real PWR.
The fission plate, the thermal shield, the pressure vessel and the void box were perfectly orthogonally aligned and centred along an imaginary line Z (horizontal or nuclear axis) passing through the centre of the fission plate. Along this nuclear axis three types of threshold detectors were located in ten positions and gave the integral measurements.

The Rh-103(n,n')Rh-103m, In-115(n,n')In-115m and S-32(n,p)P-32 threshold dosimeters were employed in the PCA-Replica experiment. In practice, the results coming from Rh-103(n,n') and In-115(n,n') are comparable with neutron fluxes above about 1.0 MeV and the results from S-32(n,p) with neutron fluxes above about 3.0 MeV.
Moreover, spectral measurements were performed in two positions: in the one-quarter thickness (T) of the reactor pressure vessel (1/4 T PV) simulator and in the void box.

The PCA-Replica 12/13 experiment was simulated (see Fig. 5) with a P_3-S_8 transport calculation in (X,Y,Z) Cartesian coordinates, describing the whole integral experiment geometry and adopting a precise heterogeneous fission neutron source distribution in the fission plate.

The dosimetric results obtained in the PCA-Replica 12/13 calculations were compared with the corresponding experimental values in Figs. 6, 7 and 8 while the comparisons of calculated and experimental neutron spectra, respectively at one-quarter thickness of the pressure vessel simulator and in the void box simulating the reactor cavity beyond the pressure vessel, are shown in Figs. 9 and 10, respectively.

As far as the VENUS-3 experiment is concerned, three-dimensional fixed source transport calculations were performed with the three-dimensional TORT-3.2 discrete ordinates (S_N) code with a P_3-S_8 transport calculation in (R,Θ,Z) cylindrical coordinates, describing one-quarter of the VENUS-3 experimental reactor (see Figs. 11 and 12).

The VENUS-3 low-flux neutron shielding benchmark experiment is closely related to LWR-PV safety. It was designed to test the accuracy of the nuclear data and transport codes in the calculation of the neutron radiation damage parameters in stainless steel reactor components, in a context of great precision of the experimental results. Among the available experiments, the VENUS-3 configuration offers the exceptional advantage of exhibiting a realistic radial core shape and a typical PWR neutron spectrum. VENUS-3 was conceived taking into account that, for some early built reactors, it was proposed to reduce the lead factor at the level of the PV horizontal welding by loading Partial Length Shielded Assemblies (PLSA) at the most critical corners of the core periphery (the shielded part was obtained by replacing part of the fuel length by a stainless steel rod). VENUS-3 was addressed to test this improvement, introducing a PLSA region in the core, and to permit the validation of the analytical methods needed to predict the azimuthal variation of the fluence in the pressure vessel.
Starting from the centre, the core quadrant between 0° and 90° may be divided in the following 10 horizontal radial regions:

- the CENTRAL HOLE (water);
- the INNER BAFFLE (stainless steel thickness: 2.858 cm);
- the 4/0 FUEL REGION: 4% enriched uranium fuel rods and 11 pyrex control rods, typical of PWR poison clusters;
- the 3/0 FUEL REGION: 3.3% enriched uranium fuel rods and PLSA rods;
- the OUTER BAFFLE (stainless steel thickness. 2.858 cm);
- the REFLECTOR (water minimum thickness: 2.169 cm);
- the BARREL (stainless steel thickness: 4.99 cm);
- the WATER GAP (water thickness: 5.80 cm);
- the NEUTRON PAD (stainless steel average thickness: 6.72 cm);
- the VENUS environment, i.e., the jacket (air filled), the reactor vessel (stainless steel) and the reactor room (air).

The In-115(n,n')In-115m, Ni-58(n,p)Co-58 and Al-27(n,α)Na-24 threshold dosimeters were employed in the VENUS-3 experiment. In practice the results coming from In-115(n,n') are comparable with neutron fluxes above about 1.0 MeV, the results from Ni-58(n,p) with neutron fluxes above about 3.0 MeV and the results from Al-27(n,α) with neutron fluxes above about 8.0 MeV.
In the VENUS-3 experiment the total number of the dosimeters is 386: the In-115(n,n') dosimeters are in 104 positions, the Ni-58(n,p) dosimeters are in 244 positions and the Al-27(n,α) dosimeters are in 38 positions. In other words, each set of dosimeters is placed in a part of the 268 total different spatial locations. Axially, the dosimeters are located at 14 different axial levels between 105.0 cm and 155.0 cm, respectively the lower height and the upper height of the active core region (see Fig. 12).

The dosimetric results obtained in the VENUS-3 calculations were compared with the corresponding experimental values in Figs. 13, 14 and 15.

It is worth pointing out that in both the PCA-Replica 12/13 and VENUS-3 calculations, the deviations of the dosimetric results from the corresponding experimental data were contained within ± 10 %, as officially recommended.

Finally, the ENEA-Bologna data processing and validation activities addressed to produce and to test the ENEA-Bologna MATJEFF31.BOLIB fine-group (199 neutron groups + 42 photon groups) coupled neutron and photon cross section library in MATXS format for nuclear fission applications, based on the JEFF-3.1/JEFF-3.1.1 evaluated nuclear data, were cited in Ref. [C.10].

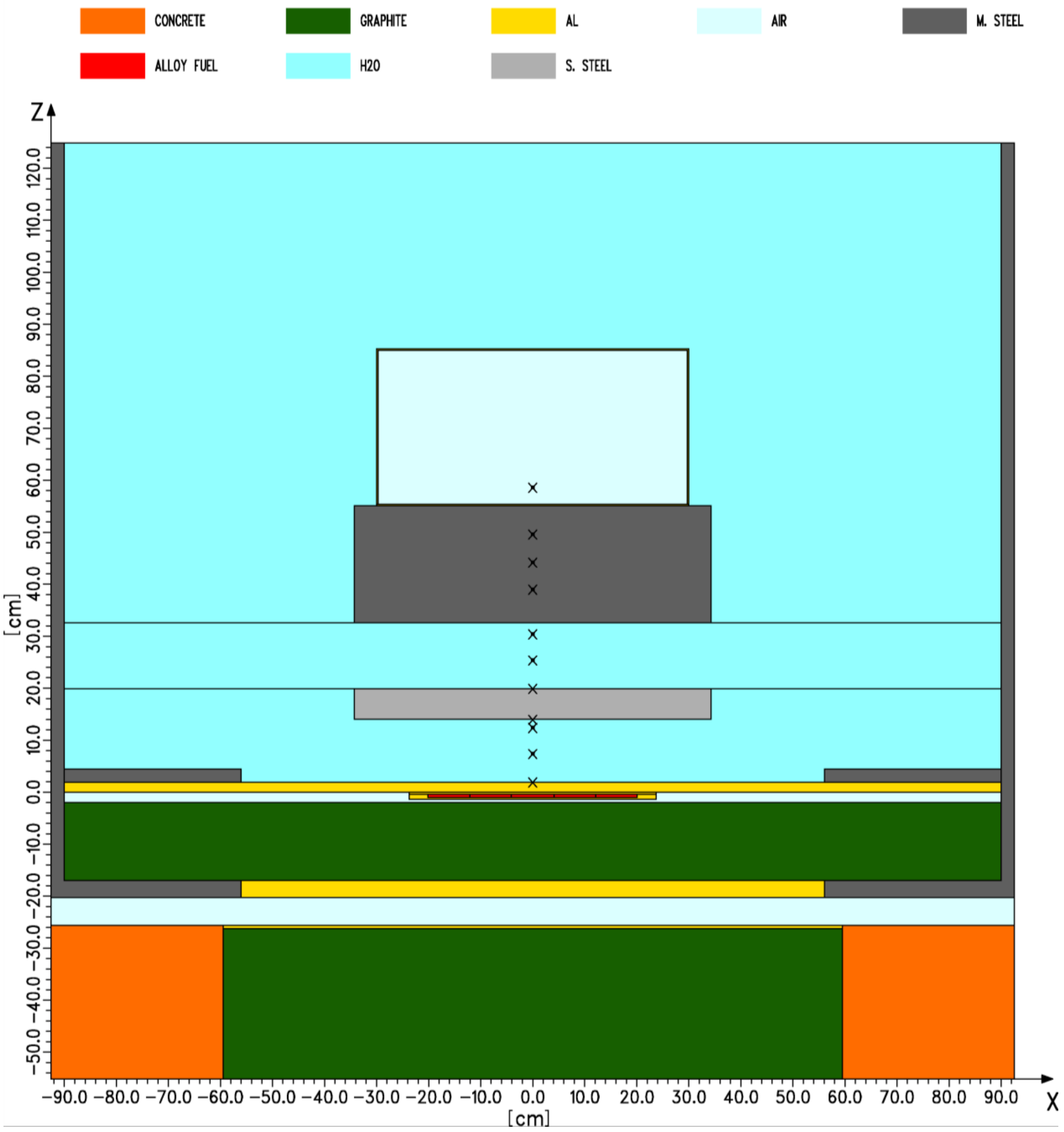

Fig. 5. PCA-Replica Model with TORT-3.2 (X,Y,Z), Horizontal Section at Y=0.0 cm. Dosimeter Locations “×”, 65X×63Y×182Z Spatial Meshes.

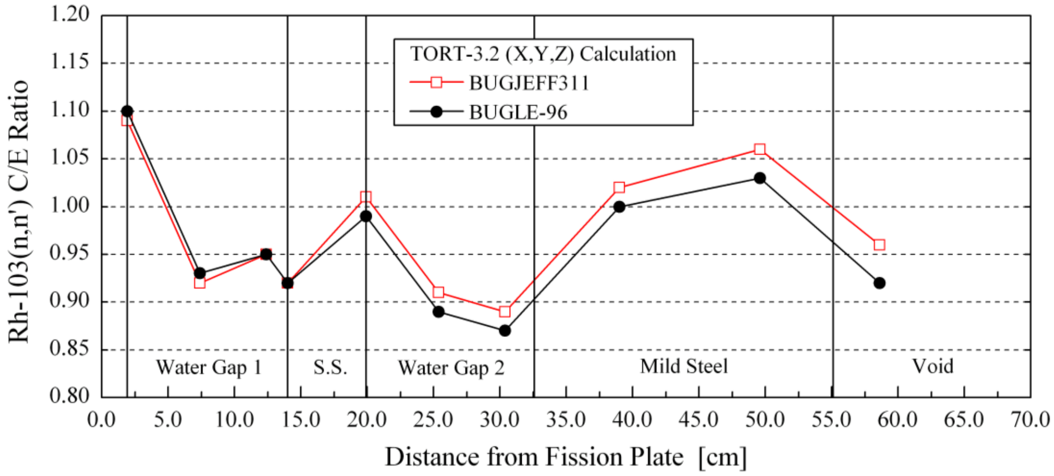

Fig. 6. PCA-Replica - Rh-103(n,n') Reaction Rates Ratios (Calculated/Experimental).

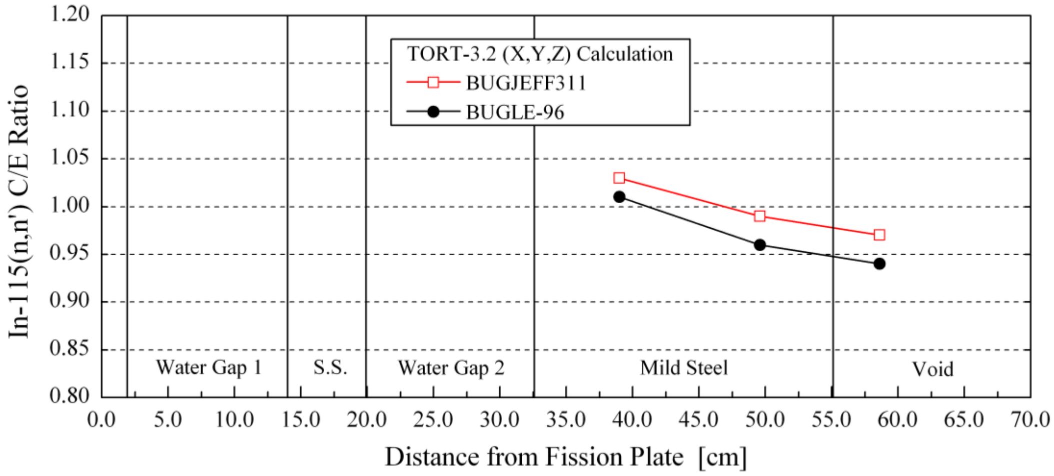

Fig. 7. PCA-Replica - In-115(n,n') Reaction Rates Ratios (Calculated/Experimental).

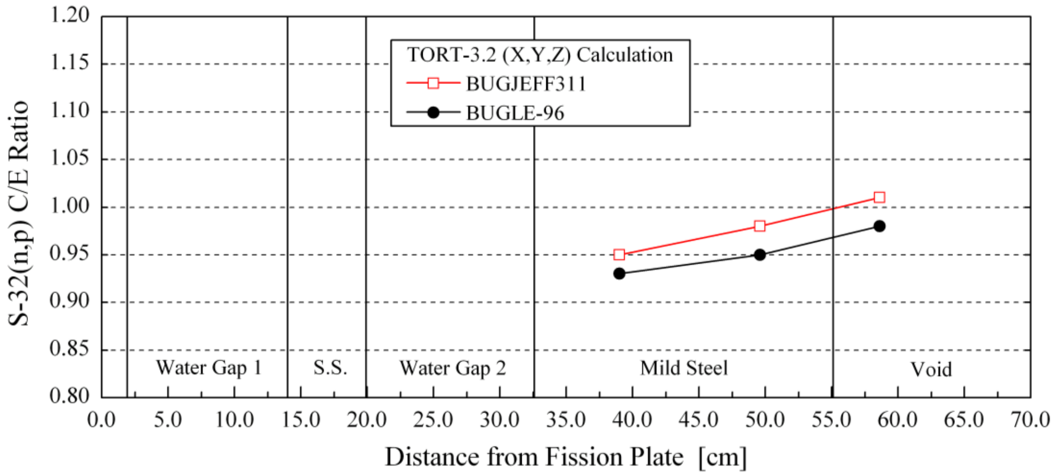

Fig. 8. PCA-Replica - S-32(n,p) Reaction Rates Ratios (Calculated/Experimental).

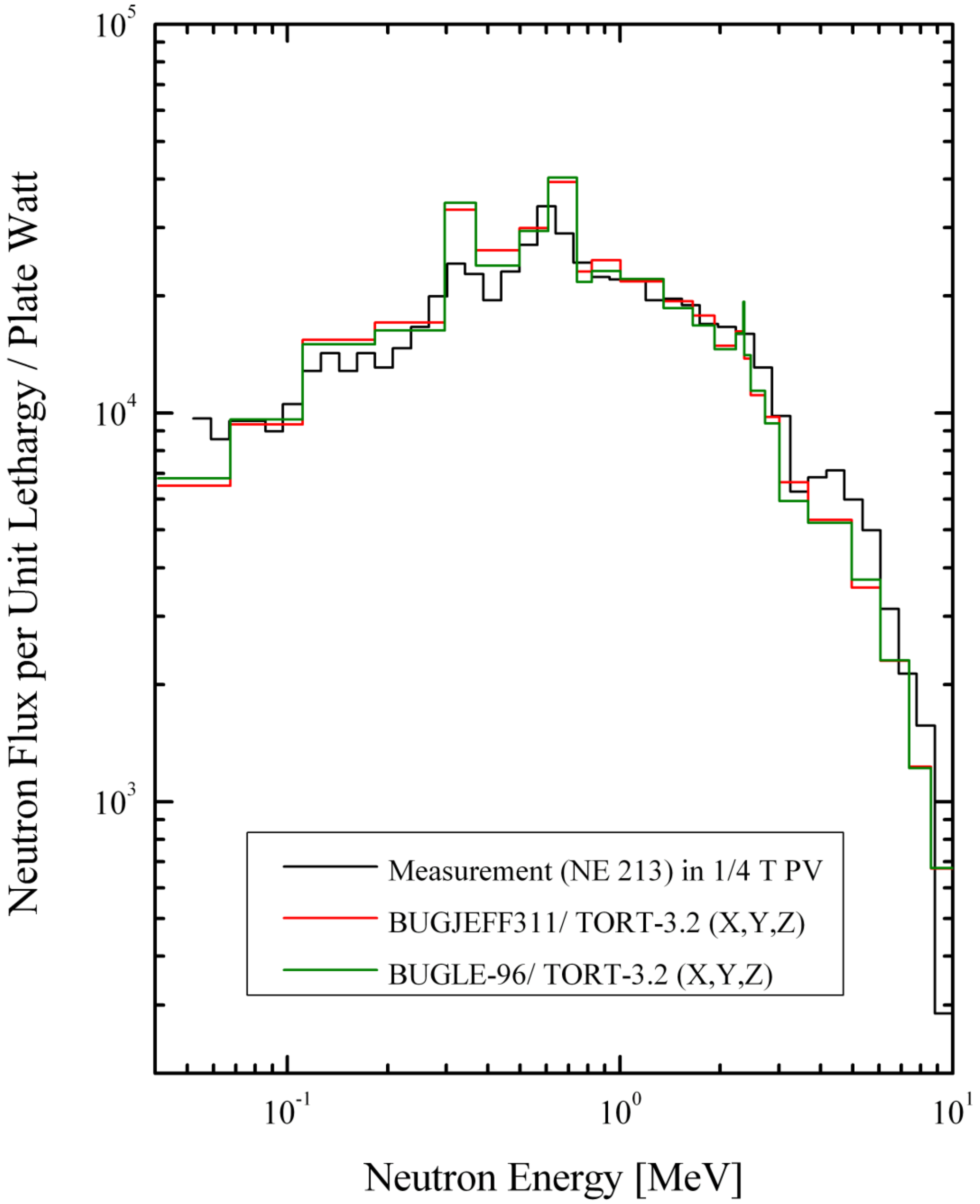

Fig. 9. PCA-Replica - Comparison of Experimental and Calculated Neutron Fluxes in the RPV 1/4 T Position (Mild Steel).

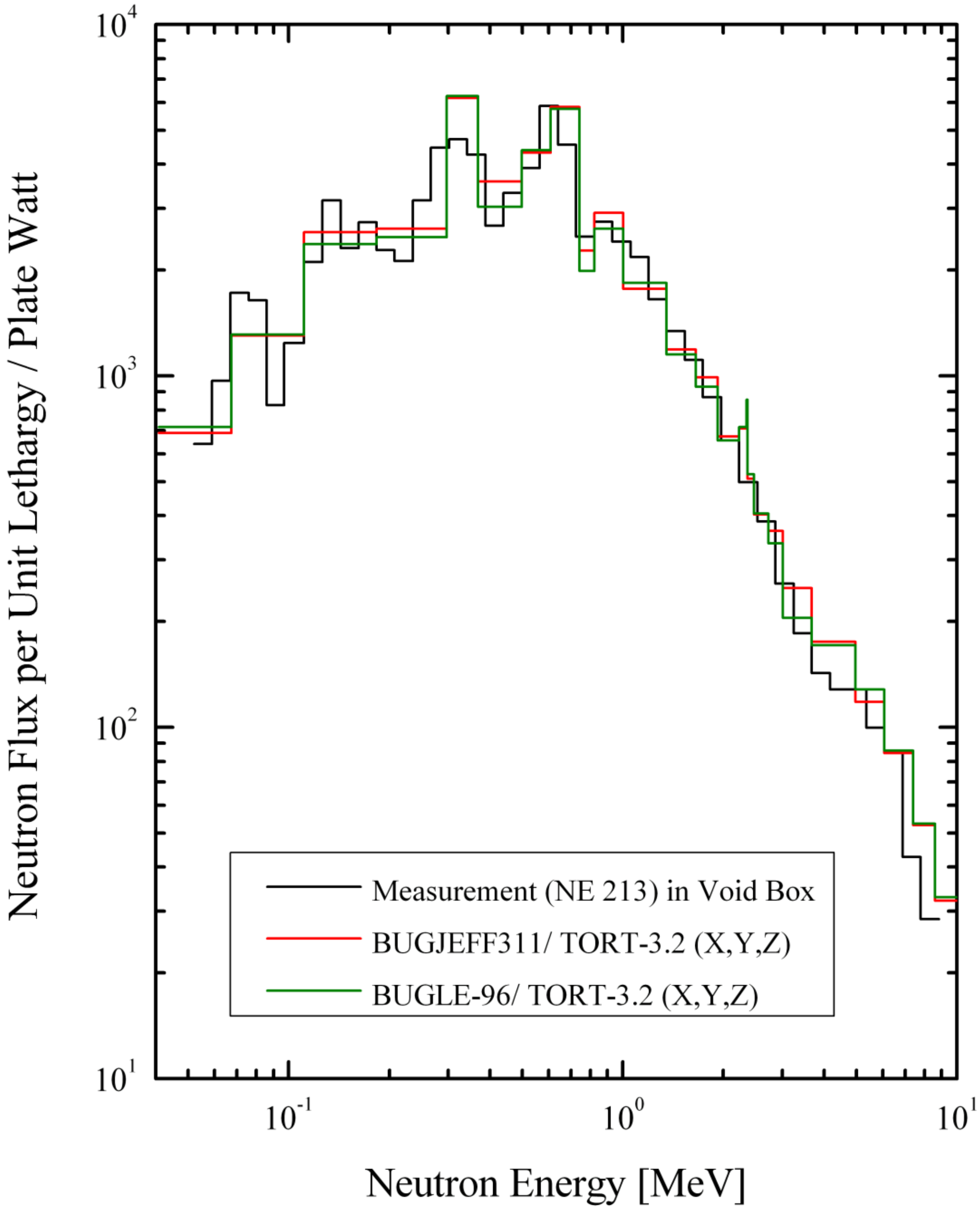

Fig. 10. PCA-Replica - Comparison of Experimental and Calculated Neutron Fluxes in the Void Box Position (Air).

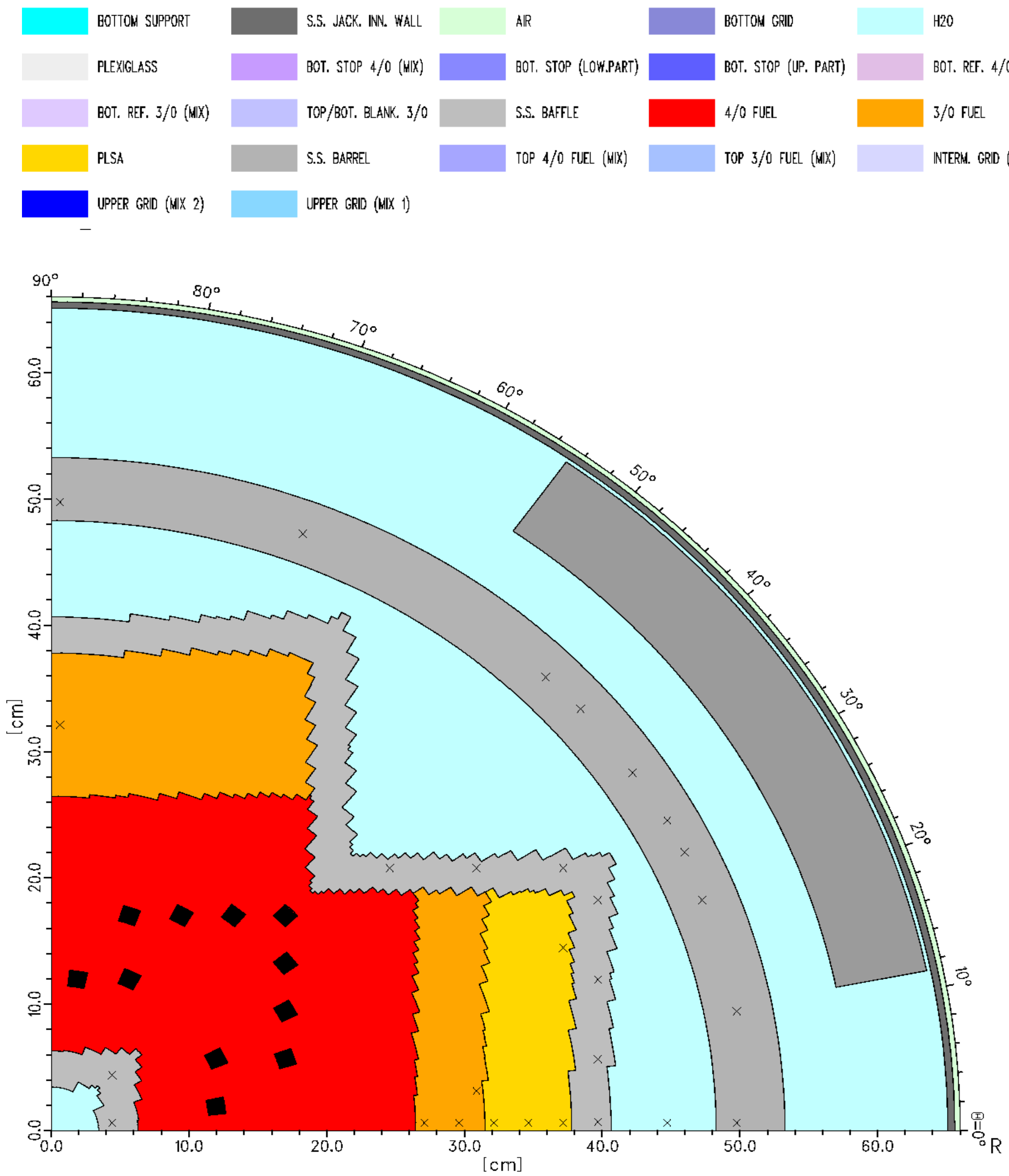

Fig. 11. VENUS-3 Model with TORT-3.2 (R,Θ,Z), Horizontal Section at Z=114.50 cm. Dosimeter Locations "×", 111R×113Θ×71Z Spatial Meshes.

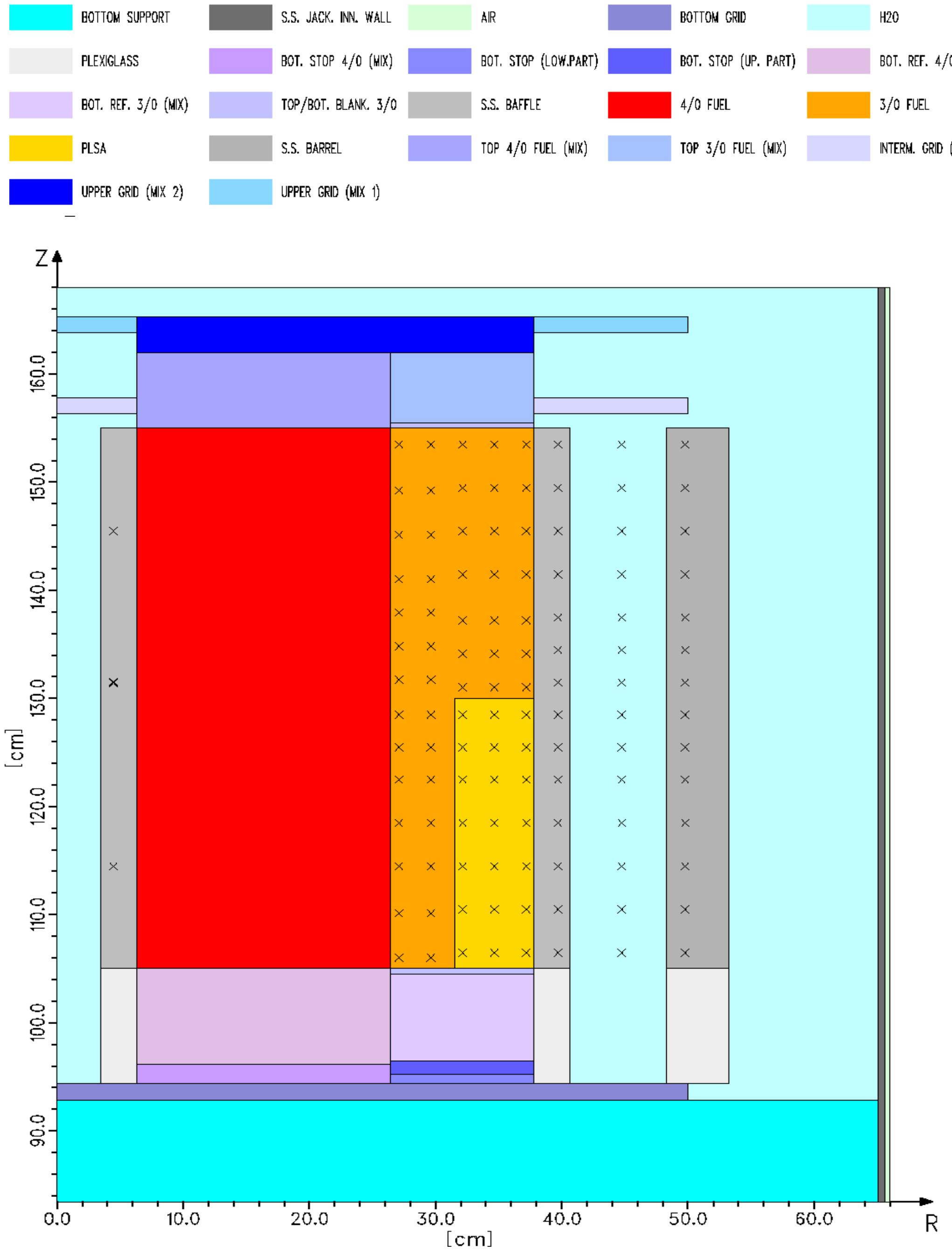

Fig. 12. VENUS-3 Model with TORT-3.2 (R,Θ,Z), Vertical Section at Θ=0°. Dosimeter Locations “×”, 111R×113Θ×71Z Spatial Meshes.

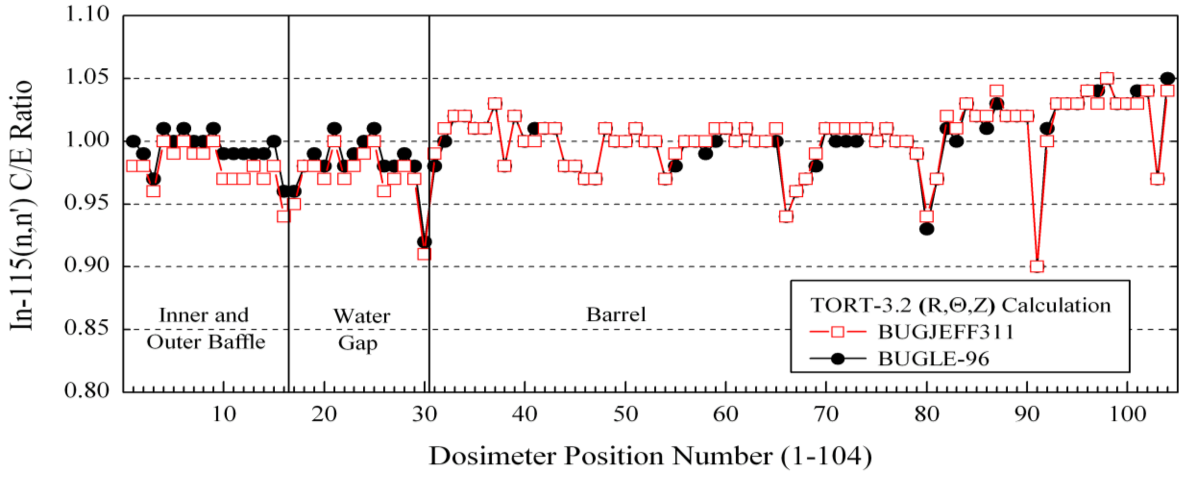

Fig. 13. VENUS-3 - In-115(n,n') Equivalent Fission Flux Ratios (Calculated/Experimental).

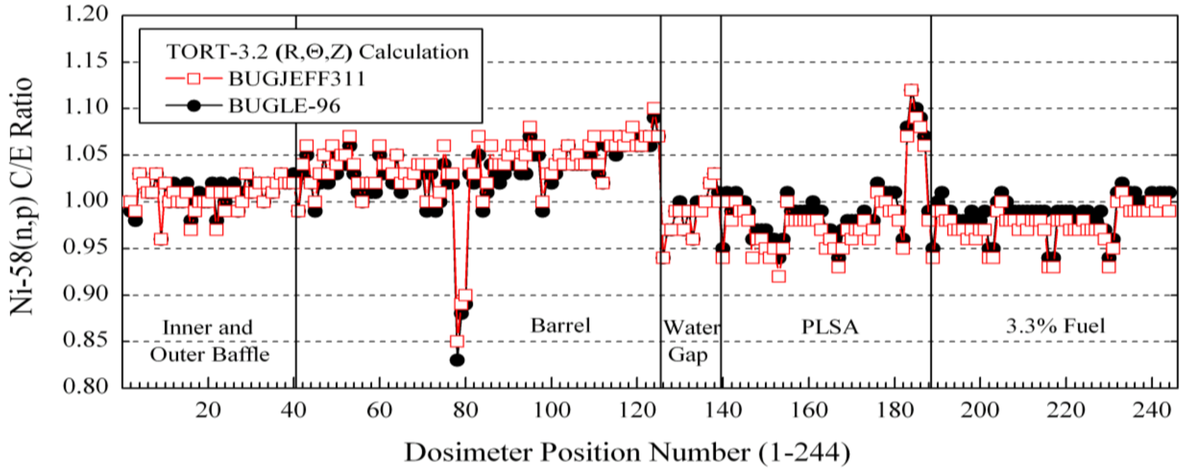

Fig. 14. VENUS-3 - Ni-58(n,p) Equivalent Fission Flux Ratios (Calculated/Experimental).

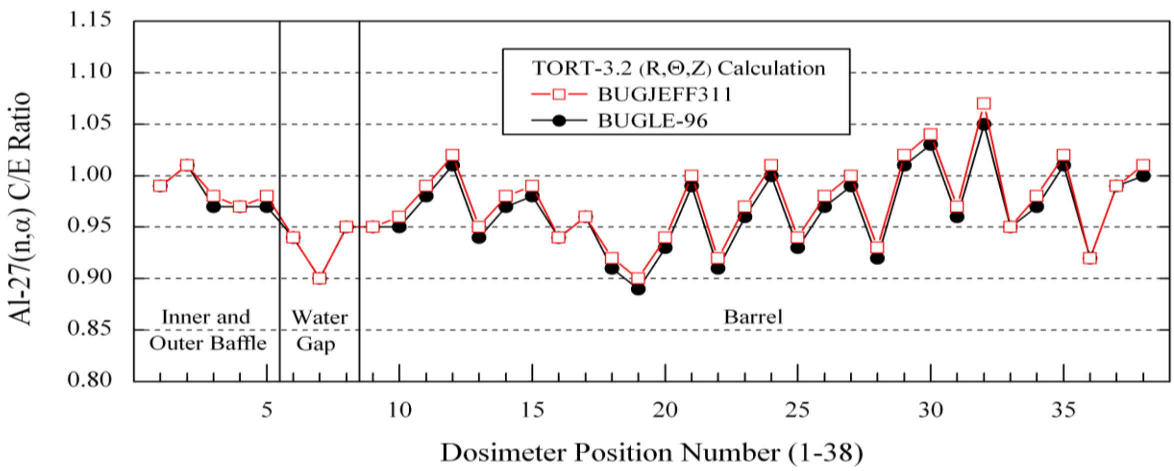

Fig. 15. VENUS-3 - Al-27(n,α) Equivalent Fission Flux Ratios (Calculated/Experimental).

Computer Code Development

The pre/post-processor code system BOT3P was updated and improved by adding new options, according to the users' feedback, leading to the BOT3P Version 5.5.

BOT3P is a set of standard FORTRAN 77 language codes developed at the ENEA-Bologna Nuclear Data Group and is designed to run on Linux/UNIX platforms. BOT3P Version 1.0 was originally conceived as a set of standard FORTRAN 77 language programs in order to give to the users of the two-dimensional (2D) DORT and three-dimensional (3D) TORT discrete ordinates transport codes of the ORNL DOORS system of deterministic codes (distributed by OECD-NEA Data Bank) some useful calculation tools to prepare and check their input data files. In particular BOT3P contains modules that automatically generate the spatial mesh grids for both Cartesian and cylindrical geometries in two-dimensions and three-dimensions, using a combinatorial geometry methodology to describe complicated 2D and 3D input geometries. Moreover BOT3P allows the check of the input geometrical models and the visualization of the results through graphical modules that perform 2D cuts and 3D views.

Later versions of BOT3P extended the possibility to produce geometrical, material distribution and neutron fixed source data to other deterministic transport codes such as TWODANT and THREEDANT (both included in the LANL DANTSYS package of deterministic codes), PARTISN (the LANL updated parallel version of DANTSYS distributed by OECD-NEA Data Bank), the sensitivity code SUSD3D (distributed by OECD-NEA Data Bank) and potentially to any transport code, through BOT3P binary output files that can be very easily interfaced. See, for example, the Westinghouse Electric Co. parallel discrete ordinates transport code RAPTOR-M3G (RApid Parallel Transport Of Radiation-Multiple 3D Geometries) and the Russian two and three-dimensional neutron, photon and charged particle discrete ordinates transport codes KASKAD-S-2.5 and KATRIN-2.0, included in the CNCSN 2009 system of deterministic codes (distributed by OECD-NEA Data Bank).

BOT3P allows users to model (X,Y), (X,Z), (Y,Z), (R,Θ) and (R,Z) geometries in two dimensions and (X,Y,Z) and (R,Θ,Z) geometries in three dimensions.

BOT3P was systematically and successfully used in 2010 in ENEA to generate the R-Θ-Z geometrical models in the IRIS (International Reactor Innovative and Secure) shielding analysis of the vessel by deterministic methods.
The IRIS application involved larger and larger models (several million spatial cells) and particular features were required by this application. Some of these new features are now permanently included in BOT3P Version 5.5. Moreover a few corrections in the RVARSCL module (TORT post-processor) of BOT3P were necessary to solve errors detected by some users.

A more efficient module to produce tetrahedron mesh grids starting from voxelized geometries, which might be particularly useful in medical applications, is in development and will probably be included in a next BOT3P release.

BOT3P has got large world-wide diffusion and is currently used by important companies such as, for example, Westinghouse Electric Co. and Ansaldo Nucleare and BOT3P Version 5.3 is currently available from both OECD/NEA Data Bank and ORNL-RSICC:

- NEA-1678 BOT3P-5.3 BOT3P5.3, 3D Mesh Generator and Graphical Display of Geometry for Radiation Transport Codes, Display of Results.

- RSICC CODE PACKAGE PSR-530: BOT3P-5.3: Code System for 2D and 3D Mesh Generation and Graphical Display of Geometry and Results for Radiation Transport Codes.

Publications 2010

Articles

[A.1] G.A. Kerimov and A. Ventura, *Group-theoretical approach to a non-central extension of the Kepler-Coulomb problem,* J. Phys. A: Math. Theor. **43**, 255304 (2010).

[A.2] F. Cannata and A. Ventura, *Reflectionless PT-symmetric potentials in the one-dimensional Dirac equation,* J. Phys. A: Math. Theor. **43**, 075305 (2010).

[A.3] The n_TOF Collaboration: G. Tagliente, P.M. Milazzo, K. Fujii, U. Abbondanno, G. Aerts, H. Alvarez, F. Alvarez-Velarde, S. Andriamonje, J. Andrzejewski, L. Audouin, G. Badurek, P. Baumann, F. Bečvár, F. Belloni, E. Berthoumieux, S. Bisterzo, F. Calviño, M. Calviani, D. Cano-Ott, R. Capote, C. Carrapiço, P. Cennini, V. Chepel, E. Chiaveri, N. Colonna, G. Cortes, A. Couture, J. Cox, M. Dahlfors, S. David, I. Dillmann, C. Domingo-Pardo, W. Dridi, I. Duran, C. Eleftheriadis, M. Embid-Segura, A. Ferrari, R. Ferreira-Marques, W.Furman, R. Gallino, I. Goncalves, E. Gonzalez-Romero, F. Gramegna, C. Guerrero, F. Gunsing, B. Haas, R. Haight, M. Heil, A. Herrera-Martinez, M. Igashira, E. Jericha, F. Käppeler, Y. Kadi, D. Karadimos, D. Karamanis, M. Kerveno, E. Kossionides, M. Krtička, C. Lamboudis, H. Leeb, A. Lindote, I. Lopes, M. Lozano, S. Lukic, J. Marganiec, S. Marrone, T. Martinez, C. Massimi, P. Mastinu, A. Mengoni, C. Moreau, M. Mosconi, F. Neves, H. Oberhummer, S. O'Brien, J. Pancin, C. Papachristodoulou, C. Papadopoulos, C. Paradela, N. Patronis, A. Pavlik, P. Pavlopoulos, L. Perrot, M.T. Pigni, R. Plag, A. Plompen, A. Plukis, A. Poch, J. Praena, C. Pretel, J. Quesada, T. Rauscher, R. Reifarth, M. Rosetti, C. Rubbia, G. Rudolf, P. Rullhusen, J. Salgado, C. Santos, L. Sarchiapone, I. Savvidis, C. Stephan, G. Tagliente, J. L. Tain, L. Tassan-Got, L. Tavora, R. Terlizzi, G. Vannini, P. Vaz, A. Ventura, D. Villamarin, M.C. Vincente, V. Vlachoudis, R. Vlastou, F. Voss, S. Walter, M. Wiescher and K. Wisshak, *The $^{92}Zr(n,\gamma)$ reaction and its implications for stellar nucleosynthesis*, Phys. Rev. C **81**, 055801 (20010).

[A.4] C. Massimi *et al.* (the n_TOF Collaboration), *$^{197}Au(n,\gamma)$ cross section in the resonance region*, Phys. Rev. C **81**, 044616 (2010).

[A.5] M. Mosconi *et al.* (the n_TOF Collaboration), *Neutron physics of the Re/Os clock. I. Measurement of the (n,γ) cross sections of $^{186,187,188}Os$ at the CERN n_TOF facility*, Phys. Rev. C **82**, 015802 (2010).

[A.6] K. Fujii *et al.* (the n_TOF Collaboration), *Neutron physics of the Re/Os clock. III. Resonance analyses and stellar (n,γ) cross sections of $^{186,187,188}Os$*, Phys. Rev. C **82**, 015804 (2010).

[A.7] C. Paradela *et al.* (the n_TOF Collaboration), *Neutron-induced fission cross section of ^{234}U and ^{237}Np measured at the CERN Neutron Time-of-flight (n_TOF) facility*, Phys. Rev. C **82**, 034601 (2010).

[A.8] N. Colonna *et al.* (the n_TOF Collaboration), *Neutron cross sections for next generation reactors: new data from n_TOF*, Appl. Rad. Is. **68**, 643 (2010).

Conference Contributions

[C.1] G.A. Kerimov and A. Ventura, *Algebraic approach to non-central potentials in the n-dimensional Schrödinger equation,* invited presentation at the 29th International Workshop on Nuclear Theory, Rila Mountains, Bulgaria, 20-26 June 2010, proceedings edited by A. Georgieva and N. Minkov, Heron Press, Sofia, 2010, p. 11.

[C.2] C. Paradela *et al.* (the n_TOF Collaboration), *^{237}Np (n,f) cross section: new data and present status*, Proceedings of the International Conference on Nuclear Data for Science and Technology (ND-2010), Jeju Island, Korea, April 26-30, 2010 , J. Kor. Phys. Soc. **59**, 1908 (2011).

[C.3] E. Chiaveri *et al.* (the n_TOF Collaboration) , *Past, present and future of the n_TOF facility at CERN,* Proceedings of the International Conference on Nuclear Data for Science and Technology (ND-2010), Jeju Island, Korea, April 26-30, 2010, J. Kor. Phys. Soc. **59**, 1620 (2011).

[C.4] C. Guerrero *et al.* (the n_TOF Collaboration), *Characterization of the new n_TOF beam: fluence, profile and resolution*, Proceedings of the International Conference on Nuclear Data for Science and Technology (ND-2010), Jeju Island, Korea, April 26-30, 2010, J. Kor. Phys. Soc. **59**, 1624 (2011).

[C.5] E. Mendoza *et al.* (the n_TOF Collaboration), *Improved neutron capture cross section measurements with the n_TOF total absorption calorimeter,* Proceedings of the International Conference on Nuclear Data for Science and Technology (ND-2010), Jeju Island, Korea, April 26-30, 2010, J. Kor. Phys. Soc. **59**, 1813 (2011).

[C.6] C. Guerrero *et al.* (the n_TOF Collaboration), *Study of photon strength function of actinides: the case of ^{235}U, ^{238}Np, and ^{241}Pu,* Proceedings of the International Conference on Nuclear Data for Science and Technology (ND-2010), Jeju Island, Korea, April 26-30, 2010, J. Kor. Phys. Soc. **59**, 1510 (2011).

[C.7] D. Cano-Ott *et al.* (the n_TOF Collaboration), *Neutron capture measurements on minor actinides at the n_TOF facility at CERN: past, present and future,* Proceedings of the International Conference on Nuclear Data for Science and Technology (ND-2010), Jeju Island, Korea, April 26-30, 2010, J. Kor. Phys. Soc. **59**, 1809 (2011).

[C.8] M. Calviani *et al.* (the n_TOF Collaboration), *Fission cross section measurements of ^{233}U, ^{245}Cm and ^{241,243}Am at the CERN n_TOF facility*, Proceedings of the International Conference on Nuclear Data for Science and Technology (ND-2010), Jeju Island, Korea, April 26-30, 2010, J. Kor. Phys. Soc. **59**, 1912 (2011).

[C.9] D. Tarrio *et al.* (the n_TOF Collaboration), *High-energy neutron-induced fission cross sections of natural lead and ^{209}Bi,* Proceedings of the International Conference on Nuclear Data for Science and Technology (ND-2010), Jeju Island, Korea, April 26-30, 2010, J. Kor. Phys. Soc. **59**, 1904 (2011).

[C.10] A.J. Koning, E. Bauge, C.J. Dean, E. Dupont, U. Fischer, R.A. Forrest, R. Jacqmin, H. Leeb, M.A. Kellet, R.W. Mills, C. Nordborg, M. Pescarini, Y. Rugama, P. Rullhusen, *Status of the JEFF Nuclear Data Library*, Proceedings of the International Conference on Nuclear Data for Science and Technology (ND-2010), Jeju Island, Korea, April 26-30, 2010, J. Kor. Phys. Soc., **59**, 1057 (2011). Published also as ENEA Technical Report UTFISSM-P9H6-001, July 8, 2010.

Project Staff

Dr. Manuela Frisoni

Dr. Roberto Orsi

Dr. Massimo Pescarini

Dr. Alberto Ventura

Nuclear Data Section
International Atomic Energy Agency
P.O. Box 100
A-1400 Vienna
Austria

e-mail: services@iaeand.iaea.org
fax: (43-1) 26007
telephone: (43-1) 2600-21710
Web: http://www-nds.iaea.org